Acta Chemica Scandinavica A 36 (1982) 783–795

Compounds with Intermediate Spin. 6.* Structure and Magnetic Properties of Tris(*N*,*N*-dipropionitriledithiocarbamato)iron(III) Hemichloroform

J. ALBERTSSON, Å. OSKARSSON and K. STÅHL

Inorganic Chemistry 1 and 2, Chemical Center, University of Lund, P.O.B. 740, S-220 07 Lund, Sweden

$Fe[S_2CN(C_3H_4N)_2]_3 \cdot \frac{1}{2}CHCl_3$, $M_r = 710.38$, has a temperature dependent magnetic moment which varies from $\mu_{eff} = 1.50$ at 5 K to 4.09 at 315 K. Its crystal structure has been determined with direct and Fourier methods from X-ray intensities collected with a four-circle single-crystal diffractometer at 210 and 297 K. At both temperatures the crystals are triclinic with space group $P\bar{1}$, $Z = 2$; $a = 10.676(4)$, $b = 12.038(5)$, $c = 14.034(5)$ Å, $\alpha = 70.36(4)$, $\beta = 74.61(3)$, $\gamma = 67.26(3)°$, $V = 1547(1)$ Å^3, $D_x = 1.525$ g cm^{-3} and $\mu_{eff} = 3.19$ at 210 K; $a = 10.756(5)$, $b = 12.062(6)$, $c = 14.113(6)$ Å, $\alpha = 70.14(5)$, $\beta = 74.98(3)$, $\gamma = 67.59(4)°$, $V = 1574(1)$ Å^3, $D_x = 1.499$ g cm^{-3} and $\mu_{eff} = 3.94$ at 297 K. The least-squares refinements converged to $R = 0.048$ (210 K) and 0.061 (297 K). The structure comprises mononuclear complexes of pseudosymmetry D_3. They are van der Waals packed with statistically distributed chloroform molecules. The magnetic properties were investigated with the Faraday method in the temperature range 5–315 K using a microcomputer controlled balance together with $N_2(l)$ and He(l) cryostats. Above 225 K, the effective changes of enthalpy and entropy for the low to high-spin transition can be obtained from a ln K *vs.* T^{-1} plot: $\Delta H_{eff} = 8.4(3)$ kJ mol^{-1}, $\Delta S_{eff} = 22(1)$ J K^{-1} mol^{-1}. The spin transition appears to be non-cooperative.

Most complexes formed between iron(III) and substituted dithiocarbamate ligands have properties that are characteristic of a thermal equilibrium between the low-spin $^2T_2$ and high-spin $^6A_1$ states of iron(III) (assuming O_h symmetry of the FeS_6 core).[1,2] The present series of investigations [3,4] aims at correlating the magnetic behaviour of various $Fe(S_2CNR_2)_3$ complexes with their geometrical features: (*i*) the size, symmetry and distortion of the FeS_6 core at different temperatures, (*ii*) bond distances, bond angles and conformations of the ligand molecules, especially the S_2CNC_2 part, and (*iii*) the crystal packing of the complexes. Thermal smearing prevents the resolution of high and low-spin complexes except at very low temperatures,[5] but there are still relatively large changes in the geometry of the FeS_6 core between the two spin states since the difference between the high and low-spin radii of Fe^{3+} is about 0.15 Å.[4] Thus the spin transition may readily be affected by changes in the structure as the crystal must be able to accommodate the two types of complex simultaneously.

It has been suggested that the transformation from high to low-spin would involve the formation of small regions of low-spin complexes in a high spin crystallite and the subsequent growth of these low-spin domains.[6,7] In this description, crystal defects are preferred sites for nucleation of the minority spin domain, but they can also inhibit further growth by increasing the activation energy. For some materials one way to increase the number of crystal defects is to grind the sample thoroughly. Solid solvates may have additional crystal defects caused by disorder and loss of the solvent molecules.

In this paper we report the crystal structure of tris(*N*,*N*-dipropionitriledithiocarbamato)iron(III) hemichloroform at 210 and 297 and its magnetic properties in the temperature range 5–315 K. The propionitrile substituent was chosen because the

* For part 5 in this series see Ref. 4.

0302-4377/82/100783-13$02.50

corresponding secondary amine has a smaller pK_a value than those corresponding to the other substituents we have investigated: $pK_a \approx 5.3$ for dipropionitrile amine in aqueous solution[8] as compared to 10.9 for dimethylamine.[9] Thus, there might be a change in the FeS_2CN part of the complex caused by the changed inductive effect of the substituents on the nitrogen atom.

EXPERIMENTAL

An ethanol solution with 0.1 mol l^{-1} sodium *N,N*-dipropionitriledithiocarbamate was prepared by mixing equal amounts of carbon disulfide, dipropionitrile amine and sodium hydroxide:

$$CS_2 + HN(C_3H_4N)_2 + NaOH \rightarrow Na^+ + S_2CN(C_3H_4N)_2^- + H_2O$$

The Fe(III) complex was precipitated by adding an ethanol solution of anhydrous $FeCl_3$. Black, platelike single-crystals were grown from a chloroform solution of the precipitate by slow evaporation at room temperature. All preparative work was made in nitrogen atmosphere.

Preliminary Weissenberg photographs at 295 K indicated the Laue class $\bar{1}$ and other photographs at 120 K revealed that there is no phase transition on cooling. Cell dimensions (Table 1) were derived by least squares from 50 reflexions measured with graphite monochromated Mo$K\alpha$ radiation on a CAD4 diffractometer ($\lambda\alpha_1 = 0.70930$ Å). The diffractometer was equipped with a gas-stream apparatus working with $N_2(l)$.[10] The single-crystal used was tabular c and bound by the forms {320} and {2$\bar{1}$0}. The size was $0.27 \times 0.34 \times 0.06$ mm^3. Almost full spheres of reciprocal space with radii $\sin\theta/\lambda = 0.60$ Å^{-1} were then measured at 210 and 297 K.* The intensities were collected using $\omega - 2\theta$ scans with $\Delta\omega = 1.00° + 0.50° \tan\theta$. Maximum

* The originally intended low temperature was 150 K but due to an error in the regulating system the actual temperature became 60 K higher.

Table 1. Unit cell dimensions of $Fe(S_2CN(C_3H_4N)_2)_3 \cdot \frac{1}{2}CHCl_3$ in the interval 195–297 K.

T/K	*a*/Å	*b*/Å	*c*/Å	*α*/°	*β*/°	*γ*/°	*V*/Å^3
195	10.635(4)	12.022(7)	14.025(7)	70.34(5)	74.56(3)	67.27(3)	1538(1)
210	10.676(4)	12.038(5)	14.034(5)	70.36(4)	74.61(3)	67.26(3)	1547(1)
225	10.687(4)	12.044(6)	14.035(6)	70.37(4)	74.64(3)	67.32(3)	1551(1)
240	10.719(3)	12.036(5)	14.051(5)	70.33(4)	74.70(2)	67.29(2)	1556(1)
255	10.710(6)	12.039(9)	14.073(10)	70.28(8)	74.81(5)	67.31(5)	1558(2)
270	10.740(4)	12.050(6)	14.093(6)	70.21(4)	74.92(3)	67.35(3)	1566(1)
297	10.756(5)	12.062(6)	14.113(6)	70.14(5)	74.98(3)	67.59(4)	1574(1)

Table 2. Crystal data of $Fe(S_2CN(C_3H_4N)_2)_3 \cdot \frac{1}{2}CHCl_3$ and the least-squares refinements. Unit cell dimensions are given in Table 1.

M_r ($C_{21}H_{24}FeN_2S_6 \cdot \frac{1}{2}CHCl_3$) = 710.38		
Triclinic space group $P\bar{1}$ (No. 2), $Z = 2$		
Temperature (K)	210	297
D_x (g cm^{-3})	1.525	1.499
μ(Mo$K\alpha$) (cm^{-1})	10.36	10.18
Range of transmission factor	0.78–0.95	0.77–0.95
No. of reflexions recorded	11059	11567
No. of reflexions with $I < 2\sigma_c(I)$	3489	4329
No. of reflexions in LS refinement, *m*	3868	3786
No. of parameters refined, *n*	456	433
$R = \Sigma\|\Delta F\|/\Sigma\|F_o\|$ [a]	0.048	0.061
$R_w = [\Sigma w(\Delta F)^2/\Sigma w\|F_o\|^2]^{1/2}$	0.068	0.080
$S = [\Sigma w(\Delta F)^2/(m-n)]^{1/2}$	0.938	1.015
C_1 (weighting function)	0.030	0.048
C_2 (weighting function)	2.50	1.00

[a] $\Delta F = |F_o| - |F_c|$.

counting times of 120 (210 K) and 180 s (297 K) resulted in that most reflexions had $\sigma_c(I)/I \lesssim 0.030$ and 0.020, respectively [$\sigma_c(I)$ is based on counting statistics]. The intensities of three standard reflexions were measured every two hours. They showed no systematic variations. Corrections were made for Lorentz, polarization and absorption effects (Table 2). The crystal structure was solved using one independent half of the room temperature data but, before the refinement commenced, the intensities of each pair of centrosymmetrically related reflexions were averaged for both data sets.

Magnetic susceptibilities were measured on polycrystalline samples using the Faraday principle. The apparatus consists of a medium-sized electromagnet,[11] with constant gradient pole caps and a Cahn TG electrobalance. It is similar to a Faraday balance described by Blom and Hörlin[12] but the weighing procedure is controlled by an Intel 8080 microcomputer. Temperatures below 77 K were reached using a Leybold-Heraeus He(*l*) vaporization cryostat VNK 3 – 300. The apparatus was calibrated with $HgCo(SCN)_4$.[13] In order to check saturation effects the measurements were repeated at different field strengths, 0.6 and 0.8 T. Effects caused by crystal size and perfection were investigated by also repeating the measurements after carefully grinding the sample with agate mortar and pestle.

SOLUTION AND REFINEMENT OF THE STRUCTURE

The FeS_6 core of the complex was located with MULTAN.[14] The intensity statistics indicated a centric distribution (*i.e.* space group $P\bar{1}$). The rest of the non-H ligand atoms were found in a difference electron density map. The positions of the H atoms in the CH_2 groups were calculated assuming tetrahedral C atoms and C – H = 1.0 Å. These atoms were assigned fixed isotropic thermal parameters $B = 5.0$ Å^2 at 210 K and 8.0 Å^2 at 297 K while the other ones were assumed to vibrate anisotropically within the simple harmonic approximation. A least-squares refinement of the room temperature structure gave no better value of R than 0.13. A new difference map revealed a chloroform molecule located at either of two centrosymmetrically related positions near $\frac{1}{2},\frac{1}{2},0$. A disorder was also detected in one of the ligands. The dissordered group, $-C(6)H_2-C(7)\equiv N(3)$, was subsequently treated as statistically distributed over two sets of positions, *A* and *B*, at both temperatures.

The function $\Sigma w(\Delta F)^2$ was minimized with full-matrix least-squares refinement (Table 2). The weights w were calculated from $w^{-1} = \sigma_c^2(|F_o|) + (C_1|F_o|)^2 + C_2$ with C_1 and C_2 so adjusted that constant values of $<w(\Delta F)^2>$ were obtained in different $|F_o|$ and $\sin\theta$ intervals. Because of the large number of parameters in the structure model, the $Fe(S_2CN)_3$ group was refined separately from the non-H atoms of the ligand substituents and the chloroform molecule until all the shifts were well below their esd's. The occupancies of the chloroform molecule and of positions *A* of the disordered propionitrile group were also included. The thermal motion of the chloroform molecule had to be treated as isotropic in the room-temperature model with the same parameter assigned to each Cl atom. The thermal parameters of C(7*A*), N(3*A*), C(7*B*) and N(3*B*) at room temperature and of C(7*B*) and N(3*B*) at 210 K could not be refined. The positions of the methylene H atoms were varied in some least-squares cycles towards the end of each refinement. The final difference map of the room-temperature structure showed some peaks with height about 1 e Å^{-3} in the vicinity of the chloroform molecule but the 210 K model gave only spurious peaks of hight less than 0.6 e Å^{-3}.

Atomic scattering factors and dispersion correction factors were taken from *International Table for X-Ray Crystallography*.[15] Atomic parameters are given in Table 3. Data and final models are compared in Fig. 1 by probability plotting of ordered values of $\delta R_i = \Delta F_i/\sigma(|F_o|_i)$ *vs.* those expected for ordered normal deviates [$\sigma(|F_o|_i) = w_i^{-1/2}$].[16] The slopes and intercepts of the curves indicate that the systematic errors are small and that $\sigma(|F_o|)$ is on average rather well estimated (*cf.* the related *S* values of Table 2). The shape of the 210 K curve does though point towards some residual errors in the model or data. The observed and calculated structure amplitudes and anisotropic thermal parameters are available on request.

DESCRIPTION OF THE STRUCTURE

The structure of $Fe[S_2CN(C_3H_4N)_2]_2 \cdot \frac{1}{2}CHCl_3$ comprises mononuclear complexes of pseudosymmetry D_3 van der Waals packed with chloroform molecules. Fig. 2 shows stereoscopic pairs of drawings of the complex at 210 and 297 K. Interatomic distances and angles are given in Table 4 and some geometrical characteristics of the FeS_6 polyhedron in Table 5.

Neither the temperature nor the effective magnetic moment changes much between the two

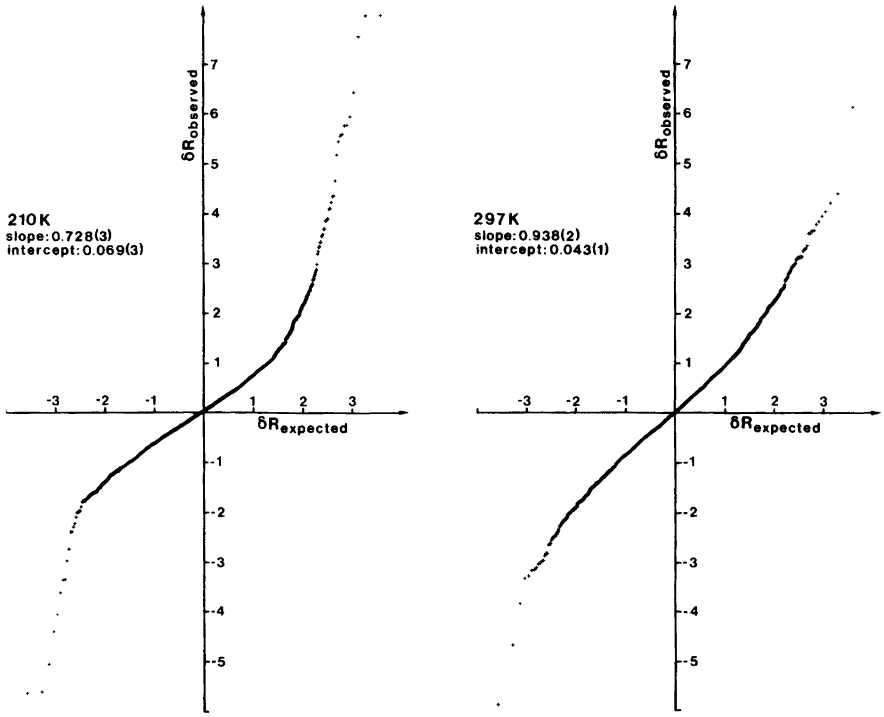

Fig. 1. δR-plot comparison of data and models of $Fe[S_2CN(C_3H_4N)_2]_3 \cdot \frac{1}{2}CHCl_3$ at 210 and 297 K.

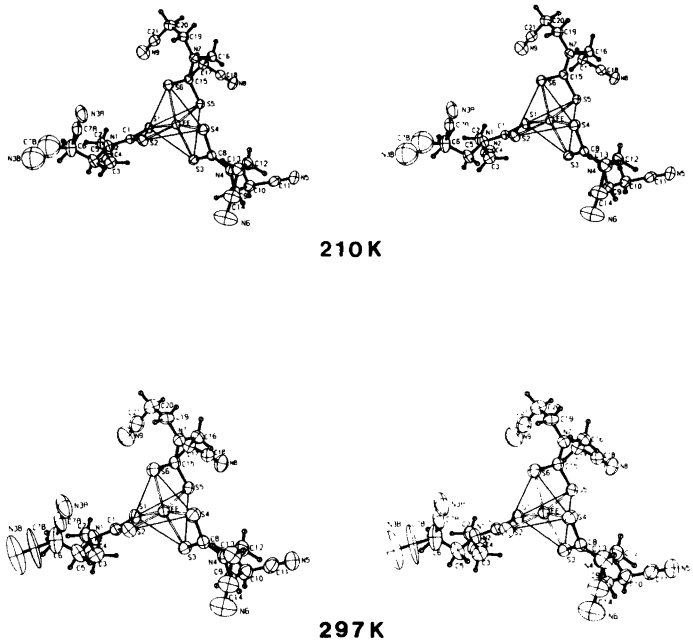

Fig. 2. Stereoscopic pairs of drawings of the complex at 210 and 297 K. The thermal ellipsoids of the non-H atoms are scaled to include 50% probability.

Table 3. Final atomic coordinates with estimated standard deviations of $Fe[S_2CN(C_3H_4N)_2]_3 \cdot \frac{1}{2}CHCl_3$. The B values of the non-H atoms were calculated from the anisotropic temperature factor coefficients. For the H atoms $B = 5.0$ Å^2 at 210 K and 8.0 Å^2 at 297 K.

	x	y	z	B/Å^2	Occupancy
(*a*) 210 K					
Fe	.31585(8)	.24787(7)	.45149(6)	2.3(1)	
S(1)	.43821(14)	.13669(14)	.33271(10)	2.5(1)	
S(2)	.16126(14)	.29665(14)	.34380(11)	2.8(1)	
C(1)	.29162(55)	.19763(51)	.27931(39)	2.4(2)	
N(1)	.28337(47)	.17048(45)	.19625(35)	2.7(2)	
S(3)	.24981(15)	.08692(14)	.57255(11)	2.7(1)	
S(4)	.15919(16)	.34128(14)	.57385(11)	3.0(1)	
C(8)	.15293(55)	.19349(56)	.64038(40)	2.6(2)	
N(4)	.08020(47)	.16779(47)	.73459(34)	2.8(2)	
S(5)	.50963(14)	.20321(13)	.52075(10)	2.4(1)	
S(6)	.39196(14)	.41618(14)	.36856(11)	2.7(1)	
C(15)	.52377(52)	.34089(49)	.43869(38)	2.2(2)	
N(7)	.62520(44)	.38387(41)	.43055(33)	2.3(1)	
C(2)	.40298(64)	.08614(59)	.14768(43)	2.9(2)	
C(3)	.41518(66)	−.04908(62)	.20620(51)	3.6(2)	
C(4)	.54683(70)	−.14029(62)	.17284(50)	3.5(2)	
N(2)	.64634(68)	−.20803(58)	.14786(52)	5.1(2)	
C(5)	.15022(69)	.20074(63)	.16606(51)	3.6(2)	
C(6)	.13012(83)	.29831(76)	.06563(54)	4.7(3)	
C(7A)	.11292(88)	.42140(81)	.07576(58)	3.5(3)	.81(2)
N(3A)	.09675(110)	.51634(106)	.08408(69)	5.5(4)	.81(2)
C(7B)	.053(10)	.381(8)	−.011(7)	12.0	.19
N(3B)	−.039(10)	.398(9)	−.045(7)	12.0	.19
C(9)	.07609(68)	.04246(69)	.78246(48)	3.7(2)	
C(10)	.19728(70)	−.04251(62)	.84113(48)	3.5(2)	
C(11)	.18799(73)	−.01128(72)	.93677(52)	4.1(3)	
N(5)	.17997(74)	.01296(71)	1.01027(45)	5.3(3)	
C(12)	.00939(62)	.26478(63)	.78985(46)	3.2(2)	
C(13)	−.12300(66)	.35480(64)	.75597(50)	3.5(2)	
C(14)	−.22369(74)	.29868(66)	.76601(62)	4.3(3)	
N(6)	−.30115(78)	.25439(72)	.76770(76)	7.3(4)	
C(16)	.72858(57)	.31253(55)	.50100(43)	2.7(2)	
C(17)	.83345(58)	.19449(57)	.46904(44)	2.8(2)	
C(18)	.87250(59)	.09147(63)	.56126(49)	3.0(2)	
N(8)	.89890(61)	.01386(56)	.63105(43)	4.1(2)	
C(19)	.63785(63)	.50008(58)	.35762(47)	3.1(2)	
C(20)	.76789(65)	.48030(61)	.27797(51)	3.4(2)	
C(21)	.78400(65)	.38849(62)	.22598(49)	3.4(2)	
N(9)	.79966(63)	.31233(67)	.18763(51)	5.0(3)	
Cl(1)	.45956(69)	.44072(71)	.11421(42)	6.1(2)	.46(1)
Cl(2)	.46609(57)	.38970(46)	−.07242(35)	6.2(2)	.46(1)
Cl(3)	.53463(102)	.60006(91)	−.08119(61)	9.2(4)	.46(1)
C(22)	.43296(161)	.50968(143)	−.01248(105)	3.9(5)	.46(1)
H(1C2)	.4845(71)	.1013(65)	.1424(52)		
H(2C2)	.4045(72)	.0979(66)	.0800(52)		
H(1C3)	.3385(70)	−.0575(65)	.1872(51)		
H(2C3)	.4172(70)	−.0573(65)	.2816(51)		
H(1C5)	.0793(71)	.2190(66)	.2258(52)		
H(2C5)	.1576(70)	.1308(65)	.1500(51)		

Table 3. Continued.

H(1AC6)	.0462	.3032	.0433		.81(1)
H(2AC6)	.2123	.2743	.0131		.81(1)
H(1BC6)	.1587	.3600	.0804		.19
H(2BC6)	.2077	.2504	.0215		.19
H(1C9)	.0787(76)	.0073(68)	.7312(55)		
H(2C9)	−.0167(76)	.0484(68)	.8363(55)		
H(1C10)	.2976(72)	−.0475(66)	.7984(52)		
H(2C10)	.2048(72)	−.1085(65)	.8544(51)		
H(1C12)	.0597(70)	.2914(66)	.7803(53)		
H(2C12)	−.0107(71)	.2201(66)	.8725(52)		
H(1C13)	−.0819(71)	.3649(66)	.6947(52)		
H(2C13)	−.1753(70)	.4150(65)	.8016(52)		
H(1C16)	.6796(71)	.2984(66)	.5567(52)		
H(2C16)	.7751(71)	.3655(66)	.4993(52)		
H(1C17)	.9131(72)	.1964(65)	.4232(51)		
H(2C17)	.7921(72)	.1668(66)	.4339(51)		
H(1C19)	.6260(71)	.5676(65)	.3925(51)		
H(2C19)	.5561(70)	.5449(65)	.3260(52)		
H(1C20)	.8643(70)	.4547(65)	.3120(51)		
H(2C20)	.7549(71)	.5685(66)	.2254(52)		
H(C22)	.3347	.5642	−.0128		.46(1)
(b) 297 K					
Fe	.31692(8)	.24666(8)	.45060(6)	3.5(1)	
S(1)	.43730(15)	.13465(15)	.33293(11)	3.9(1)	
S(2)	.16425(15)	.29602(15)	.34026(13)	4.4(1)	
C(1)	.29186(57)	.19656(53)	.27789(41)	3.6(2)	
N(1)	.28408(50)	.16997(48)	.19713(37)	4.3(2)	
S(3)	.25011(16)	.08520(14)	.57241(12)	4.2(1)	
S(4)	.16079(18)	.33989(15)	.57206(13)	4.7(1)	
C(8)	.15329(59)	.19363(56)	.63855(42)	3.8(2)	
N(4)	.08434(49)	.16577(47)	.73128(36)	4.1(2)	
S(5)	.51020(15)	.20199(14)	.52053(11)	3.9(1)	
S(6)	.39387(16)	.41603(15)	.36794(12)	4.3(1)	
C(15)	.52407(55)	.34001(50)	.43914(40)	3.4(2)	
N(7)	.62539(48)	.38173(43)	.43139(35)	3.7(2)	
C(2)	.40248(69)	.08639(60)	.14798(48)	4.4(2)	
C(3)	.41244(75)	−.04903(65)	.20434(59)	5.5(3)	
C(4)	.54057(87)	−.13725(72)	.16904(62)	5.9(3)	
N(2)	.63944(85)	−.20556(75)	.14414(71)	8.6(3)	
C(5)	.15407(78)	.20423(76)	.16253(61)	5.8(3)	
C(6)	.1380(11)	.3033(10)	.0675(7)	8.6(4)	
C(7A)	.1133(14)	.4194(11)	.0786(9)	5.7	.60(1)
N(3A)	.0918(18)	.5165(12)	.0874(11)	8.9	.60(1)
C(7B)	.0481(35)	.3499(34)	.0050(24)	15.0	.40
N(3B)	−.0317(27)	.3939(33)	−.0442(23)	14.9	.40
C(9)	.07894(69)	.04025(66)	.78115(47)	4.6(2)	
C(10)	.19710(79)	−.04411(70)	.84155(53)	5.5(3)	
C(11)	.18973(81)	−.01297(78)	.93448(60)	5.9(3)	
N(5)	.17877(98)	.01202(92)	1.00806(57)	8.8(4)	
C(12)	.01502(70)	.26216(68)	.78733(50)	4.8(2)	
C(13)	−.11661(76)	.35245(71)	.75226(62)	5.6(3)	
C(14)	−.21479(83)	.29464(73)	.76438(70)	6.1(3)	
N(6)	−.29321(92)	.25291(80)	.76718(82)	9.3(4)	
C(16)	.72717(64)	.31038(59)	.50090(50)	4.3(2)	

Table 3. Continued.

C(17)	.83207(63)	.19389(64)	.47037(49)	4.6(2)	
C(18)	.87202(65)	.09416(69)	.56073(54)	4.7(2)	
N(8)	.89986(72)	.01435(68)	.63086(52)	6.5(3)	
C(19)	.63584(68)	.49889(56)	.35897(52)	4.5(2)	
C(20)	.76426(79)	.48108(71)	.27996(59)	5.6(3)	
C(21)	.78120(85)	.38632(85)	.23085(62)	6.1(3)	
N(9)	.79982(88)	.31106(89)	.19431(69)	8.7(4)	
Cl(1)	.4499(11)	.4469(10)	.1130(8)	11.4(2)	.39(1)
Cl(2)	.4773(10)	.3927(10)	−.0691(8)	11.4(2)	.39(1)
Cl(3)	.5248(11)	.6106(10)	−.0852(8)	11.4(2)	.39(1)
C(22)	.4421(24)	.5141(24)	−.0113(19)	7.3(5)	.39(1)
H(1C2)	.4780(85)	.1085(77)	.1448(62)		
H(2C2)	.3903(86)	.1031(77)	.0755(62)		
H(1C3)	.3336(84)	−.0785(75)	.2120(62)		
H(2C3)	.4189(85)	−.0706(76)	.2902(62)		
H(1C5)	.0728(86)	.2166(77)	.2240(63)		
H(2C5)	.1299(85)	.1494(78)	.1430(63)		
H(1AC6)	.0598	.3037	.0396		.60(1)
H(2AC6)	.2163	.2837	.0151		.60(1)
H(1BC6)	.1547	.3598	.0839		.40
H(2BC6)	.2119	.2499	.0243		.40
H(1C9)	.0857(85)	−.0010(77)	.7375(63)		
H(2C9)	−.0064(85)	.0433(77)	.8271(64)		
H(1C10)	.2708(84)	−.0232(78)	.7897(62)		
H(2C10)	.1789(85)	−.1114(77)	.8561(62)		
H(1C12)	.0885(84)	.2869(77)	.7798(62)		
H(2C12)	−.0053(84)	.2106(76)	.8630(62)		
H(1C13)	−.0943(85)	.3933(76)	.6721(64)		
H(2C13)	−.1552(84)	.4073(76)	.7833(64)		
H(1C16)	.6677(83)	.2860(77)	.5675(61)		
H(2C16)	.7757(85)	.3714(77)	.4944(62)		
H(1C17)	.8903(87)	.2138(78)	.4231(62)		
H(2C17)	.7837(86)	.1623(77)	.4305(61)		
H(1C19)	.6288(84)	.5541(75)	.3881(61)		
H(2C19)	.5610(85)	.5383(77)	.3209(63)		
H(1C20)	.8582(85)	.4460(76)	.3130(61)		
H(2C20)	.7601(86)	.5618(78)	.2235(63)		
H(C22)	.3548	.5770	−.0222		.39(1)

structure determinations. The Fe−S bond distance, the S−C−S bond angle and the trigonal twist of the coordination polyhedron are strongly correlated to the effective magnetic moment as shown by an analysis of a number of accurate structure determinations (the Fe−S bond length and the S−C−S bond angle both increase while the trigonal twist decreases when μ_{eff} increases).[17] In the present structure these quantities have values expected for complexes with low μ_{eff}. The mean observed increase in the Fe−S distance between 210 and 297 K is only 0.016(1) Å while the changes in the S−C−S and twist angles are insignificant.

There are 33 bonds between non-H ligand atoms in the complex, excluding C(7*B*) and N(3*B*). The apparent bond lengths do not decrease when the temperature increases, the average decrease being 0.0038(40) Å between 210 and 297 K. Half-normal probability plotting [3,16] of $\delta d_i = \Delta d_i/\sigma(\Delta d_i)$ where Δd_i is the difference in bond lengths between the two temperatures, resulted in a correlation coefficient of 0.992, a slope of 1.35(3) and an intercept of −0.03(2). Thus the interatomic distances may have somewhat underestimated standard deviations. Another half-normal plot, this time comparing all interatomic distances less than 2.90 Å in the ligands at 210 and

Table 4. Selected interatomic distances (Å), bond angles (°) and torsion angles (°) in the $Fe[S_2CN(C_3H_4N)_2]_3$ complex and r.m.s. deviations (Å) from the least-squares planes through the S_2CNC_2 groups.

	210 K	297 K
(*a*) The FeS_6 core		
Fe–S(1)	2.295(2)	2.310(2)
Fe–S(2)	2.309(2)	2.329(2)
Fe–S(3)	2.312(2)	2.327(2)
Fe–S(4)	2.309(2)	2.324(2)
Fe–S(5)	2.317(2)	2.331(2)
Fe–S(6)	2.303(2)	2.321(2)
S(1)–S(2)	2.833(2)	2.836(3)
S(3)–S(4)	2.837(3)	2.846(3)
S(5)–S(6)	2.822(3)	2.833(3)
S(1)–S(3)	3.423(2)	3.443(3)
S(1)–S(5)	3.339(2)	3.363(2)
S(3)–S(5)	3.381(2)	3.404(3)
S(2)–S(4)	3.440(2)	3.476(3)
S(2)–S(6)	3.433(2)	3.458(3)
S(4)–S(6)	3.387(2)	3.412(3)
S(1)–S(6)	3.397(3)	3.434(3)
S(2)–S(3)	3.448(3)	3.489(3)
S(4)–S(5)	3.444(2)	3.473(3)
(*b*) Ligand 1		
S(1)–C(1)	1.707(5)	1.718(6)
S(2)–C(1)	1.718(6)	1.713(6)
C(1)–N(1)	1.344(7)	1.314(7)
N(1)–C(2)	1.458(8)	1.469(8)
C(2)–C(3)	1.528(9)	1.530(10)
C(3)–C(4)	1.484(9)	1.472(11)
C(4)–N(2)	1.114(9)	1.126(12)
N(1)–C(5)	1.466(8)	1.463(9)
C(5)–C(6)	1.505(10)	1.459(13)
C(6)–C(7A)	1.472(12)	1.379(16)
C(7A)–N(3A)	1.130(14)	1.147(18)
C(6)–C(7B)	1.396(91)	1.312(34)
C(7B)–N(3B)	1.125(132)	1.101(43)
S(1)–C(1)–S(2)	111.7(3)	111.5(3)
S(1)–C(1)–N(1)	122.7(4)	122.7(4)
S(2)–C(1)–N(1)	125.6(4)	125.8(5)
C(1)–N(1)–C(2)	120.0(5)	120.8(5)
C(1)–N(1)–C(5)	121.2(5)	121.9(5)
N(1)–C(2)–C(3)	109.7(5)	109.6(5)
C(2)–C(3)–C(4)	113.1(5)	112.1(6)
C(3)–C(4)–N(2)	179.2(7)	178.4(9)
C(2)–N(1)–C(5)	117.4(5)	116.6(5)
N(1)–C(5)–C(6)	113.2(6)	113.4(7)
C(5)–C(6)–C(7A)	110.8(6)	113.7(9)
C(6)–C(7A)–N(3A)	178.5(1.0)	179.5(1.6)
C(5)–C(6)–C(7B)	153.9(3.9)	133.0(1.8)
C(6)–C(7B)–N(3B)	141.4(9.3)	175.8(3.8)

Table 4. Continued.

S(1)–C(1)–N(1)–C(2)	−0.3(8)	−1.2(9)
S(1)–C(1)–N(1)–C(5)	166.1(5)	168.4(5)
S(2)–C(1)–N(1)–C(2)	179.0(5)	177.8(5)
S(2)–C(1)–N(1)–C(5)	−14.7(8)	−12.6(9)
C(1)–N(1)–C(2)–C(3)	81.2(7)	82.9(8)
N(1)–C(2)–C(3)–C(4)	−170.2(6)	−171.0(6)
C(1)–N(1)–C(5)–C(6)	114.0(7)	109.7(9)
N(1)–C(5)–C(6)–C(7A)	−70.2(9)	−74.0(1.2)
N(1)–C(5)–C(6)–C(7B)	−173.1(9.4)	170.1(2.5)
R.m.s. deviation	0.0366	0.0309
(*c*) Ligand 2		
S(3)–C(8)	1.701(6)	1.719(6)
S(4)–C(8)	1.727(6)	1.716(6)
C(8)–N(4)	1.346(7)	1.328(7)
N(4)–C(9)	1.443(9)	1.453(9)
C(9)–C(10)	1.541(9)	1.537(10)
C(10)–C(11)	1.481(9)	1.458(11)
C(11)–N(5)	1.137(9)	1.143(11)
N(4)–C(12)	1.467(8)	1.480(9)
C(12)–C(13)	1.491(9)	1.502(10)
C(13)–C(14)	1.431(10)	1.420(11)
C(14)–N(6)	1.136(11)	1.122(12)
S(3)–C(8)–S(4)	111.7(3)	112.0(3)
S(3)–C(8)–N(4)	125.1(5)	123.5(5)
S(4)–(8)–N(4)	123.3(5)	124.5(5)
C(8)–N(4)–C(9)	119.4(5)	121.2(5)
C(8)–N(4)–C(12)	120.6(5)	120.1(5)
N(4)–C(9)–C(10)	113.2(5)	113.6(6)
C(9)–C(10)–C(11)	113.3(6)	114.2(6)
C(10)–C(11)–N(5)	179.6(8)	177.4(9)
C(9)–N(4)–C(12)	120.1(5)	118.7(5)
N(4)–C(12)–C(13)	114.6(5)	113.8(6)
C(12)–C(13)–C(14)	114.4(6)	113.2(7)
C(13)–C(14)–N(6)	175.7(9)	175.3(1.0)
S(3)–C(8)–N(4)–C(9)	−3.2(9)	−4.3(9)
S(3)–C(8)–N(4)–C(12)	174.8(5)	173.7(5)
S(4)–C(8)–N(4)–C(9)	177.3(5)	177.7(5)
S(4)–C(8)–N(4)–C(12)	−4.8(8)	−4.4(9)
C(8)–N(4)–C(9)–C(10)	86.4(7)	87.7(8)
N(4)–C(9)–C(10)–C(11)	71.6(8)	71.3(9)
C(8)–N(4)–C(12)–C(13)	78.5(8)	77.7(8)
N(4)–C(12)–C(13)–C(14)	59.4(8)	60.9(9)
R.m.s. deviation	0.0184	0.0213
(*c*) Ligand 3		
S(5)–C(15)	1.707(9)	1.707(6)
S(6)–C(15)	1.709(5)	1.713(6)
C(15)–N(7)	1.335(7)	1.331(7)
N(7)–C(16)	1.486(7)	1.472(8)
C(16)–C(17)	1.551(8)	1.544(9)
C(17)–C(18)	1.481(9)	1.451(10)
C(18)–N(8)	1.113(9)	1.132(10)
N(7)–C(19)	1.460(8)	1.461(8)

Table 4. Continued.

C(19)–C(20)	1.527(9)	1.528(10)
C(20)–C(21)	1.453(9)	1.461(12)
C(21)–N(9)	1.151(10)	1.121(13)
S(5)–C(15)–S(6)	111.4(3)	111.8(3)
S(5)–C(15)–N(7)	124.1(4)	123.7(4)
S(6)–C(15)–N(7)	124.5(4)	124.5(4)
C(15)–N(7)–C(16)	118.8(4)	119.0(5)
C(15)–N(7)–C(19)	123.3(5)	122.2(5)
N(7)–C(16)–C(17)	111.8(5)	113.0(5)
C(16)–C(17)–C(18)	110.0(5)	110.1(6)
C(17)–C(18)–N(8)	178.4(7)	177.4(8)
C(16)–N(7)–C(9)	117.9(4)	118.8(5)
N(7)–C(19)–C(20)	113.1(5)	112.9(5)
C(19)–C(20)–C(21)	112.9(5)	112.0(6)
C(20)–C(21)–N(9)	177.4(7)	176.9(9)
S(5)–C(15)–N(7)–C(16)	−3.8(8)	−4.3(8)
S(5)–C(15)–N(7)–C(19)	178.0(5)	178.4(5)
S(6)–C(15)–N(7)–C(16)	176.2(4)	176.9(5)
S(6)–C(15)–N(7)–C(19)	−1.9(8)	−0.5(8)
C(15)–N(7)–C(16)–C(17)	76.3(7)	77.4(7)
N(7)–C(16)–C(17)–C(18)	−144.3(5)	−145.7(6)
C(15)–N(7)–C(19)–C(20)	−116.4(7)	−117.7(7)
N(7)–C(19)–C(20)–C(21)	52.1(8)	50.8(9)
R.m.s. deviation	0.0143	0.0120

297 K, was also made. For this plot the correlation coefficient is 0.997, the slope 1.47(2) and the intercept 0.01(1). We conclude that also the bond angles are quite similar at both temperatures. The dimensions of the S_2CNC_2 groups are within the ranges expected from previsouly determined dithiocarbamate structures.[17] The S–C and C–N bonds have partial double bond character indicating some degree of Fe–S π-bonding.[18] There is no evidence of any effects on these bonds caused by the ligand substituents. At both temperatures all three S_2CNC_2 groups are slightly non-planar as shown by the torsion angles and the r.m.s. deviations from the least-squares planes through them.

The C–C≡N part of the propionitrile substituents are nearly linear except the disordered C(6)–C(7)≡N(3). Excluding the latter group we find the average values C–C = 1.454(4) Å, C–N = 1.131(3) Å and C–C–N = 188.8(3)° in good agreement with the dimensions of α-acetonitrile at 215 K.[19] Acceptable dimensions are found for C(6)–C(7A)≡N(3A) but not for C(6)–C(7B)≡N(3B). There is probably a further disorder, at least of the *B* positions, as is also indicated by the large thermal parameters. Neglecting this, we can use the occupancies x_A and x_B at 210 and 297 K and calculate a formal equilibrium constant $K = x_B/x_A$ for $A \rightleftarrows B$ at both temperatures. By using eqn. (1) we

$$\ln K = -\Delta H^\circ/RT + \Delta S^\circ/R \qquad (1)$$

then estimate the order of magnitudes $\Delta H^\circ \approx 6$ kJ mol^{-1} and $\Delta S^\circ \approx 20$ J K^{-1} mol^{-1} for $A \rightleftarrows B$ (*cf.* the thermodynamic treatment of the magnetic data below).

The packing of the iron complexes and the chloroform molecules is shown in Fig. 3. Table 6 gives the dimensions of the chloroform molecule. Its occupancy converged to a value well below $\frac{1}{2}$ at room temperature but this might be an artefact caused by the strong correlation to the chlorine temperature factor. The molecules are located on either side of the symmetry centres $\frac{1}{2},\frac{1}{2},0$ resulting in overlapping electron densities. The apparent distortions are caused by this overlap.

Selected packing distances are given in Table 7. The shortest distance is about 3.04 Å, between the

Table 5. The geometry of the coordination polyhedron.

	210 K	295 K
μ_{eff}	3.19	3.94
Fe–S (Å)	2.308(3)	2.324(3)
Ligand bite (S–S) (Å)	2.831(4)	2.840(3)
Edge of riangular face (Å)	3.400(16)	3.426(17)
Height of prism (Å)	2.424(2)	2.439(3)
Torsion angle (trigonal twist) (°)	43.7(5)	43.1(4)
Tilt angle between triangular faces (°)	0.9(2)	0.8(2)
Fe – centroid of prism (Å)	0.027(2)	0.026(2)

Table 6. Bond distances (Å) and angles (°) in the chloroform molecule.

	210 K	297 K
C(22)–Cl(1)	1.739(16)	1.672(28)
C(22)–Cl(2)	1.784(16)	1.783(28)
C(22)–Cl(3)	1.716(18)	1.648(27)
Cl(1)–C(22)–Cl(2)	108.7(9)	106.9(1.5)
Cl(1)–C(22)–Cl(3)	113.3(9)	124.8(1.6)
Cl(2)–C(22)–Cl(3)	109.2(8)	108.6(1.5)

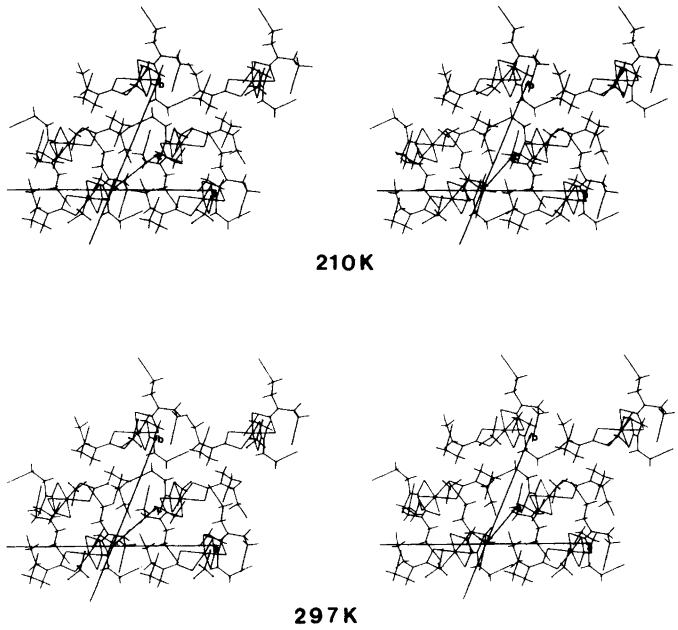

Fig. 3. Stereoscopic pairs of drawings of the crystal packing of the complexes and the chloroform molecules at 210 and 297 K. For the disordered $C(6)H_2-C(7)\equiv N(3)$ only the *A* positions are included. The chloroform molecules may also occupy centrosymmetrically related positions.

methylene C(3) and nitrile N(6) atoms. The packing of the complexes becomes more efficient when the vibration amplitudes decrease. The averaged decrease in the nitrile N contact distances is $\Delta = 0.046(5)$ Å between 297 and 210 K. The packing geometry is such that the quantity $\Delta + 2\delta(Fe-S)$

Table 7. The packing of the complexes; interatomic distances (Å) less than 3.5 Å from nitrile N atoms to atoms in neighbouring complexes and the five shortest Fe–Fe distances. The superscripts (*i*)–(*x*) denote the following transformations of the *x*, *y*, *z* values given in Table 3:

(*i*)	$1-x, \bar{y}, 1-z$	(*vi*)	$\bar{x}, \bar{y}, 1-z$
(*ii*)	$\bar{x}, 1-y, \bar{z}$	(*vii*)	$x-1, y, 1+z$
(*iii*)	$\bar{x}, 1-y, 1-z$	(*viii*)	$2-x, \bar{y}, 1-z$
(*iv*)	$x, y, z-1$	(*ix*)	$1+x, y, z$
(*v*)	$x-1, y, z$	(*x*)	$1-x, 1-y, 1-z$

	210 K	297 K
$N(2)-C(11^{i})$	3.449(10)	3.494(12)
$N(2)-N(5^{i})$	3.399(13)	3.433(13)
$N(3A)-C(6^{ii})$	3.260(13)	3.330(19)
$N(3A)-C(7A^{ii})$	3.293(13)	3.332(21)
$N(3A)-C(12^{iii})$	3.334(13)	3.375(15)
$N(3A)-C(13^{iii})$	3.246(19)	3.280(16)
$N(3B)-C(6^{ii})$	3.33(10)	3.31(4)
$N(3B)-C(7B^{ii})$	2.96(13)	3.25(5)
$N(3B)-C(12^{iv})$	3.07(9)	3.12(3)
$N(3B)-C(13^{iv})$	3.40(9)	3.47(3)
$N(3B)-N(9^{v})$	3.29(9)	3.40(3)
$N(6)-C(3^{vi})$	3.034(10)	3.053(11)
$N(6)-C(4^{vi})$	3.212(10)	3.251(12)
$N(6)-Cl(2^{vii})$	3.198(10)	3.286(14)
$N(8)-N(1^{i})$	3.436(8)	3.457(9)
$N(8)-C(5^{i})$	3.220(8)	3.295(11)
$N(8)-C(17^{viii})$	3.335(8)	3.383(10)
$N(8)-C(18^{viii})$	3.356(9)	3.400(10)
$N(9)-C(5^{ix})$	3.419(9)	3.485(12)
$N(9)-C(7B^{ix})$	3.464(9)	3.301(34)
$N(9)-C(10^{i})$	3.392(10)	3.412(12)
$Fe-Fe^{i}$	5.671(3)	5.675(4)
$Fe-Fe^{iii}$	7.294(4)	7.407(5)
$Fe-Fe^{x}$	9.001(3)	9.044(4)
$Fe-Fe^{vi}$	10.185(4)	10.208(5)
$Fe-Fe^{v}$	10.676(3)	10.756(4)

Table 7. Continued.

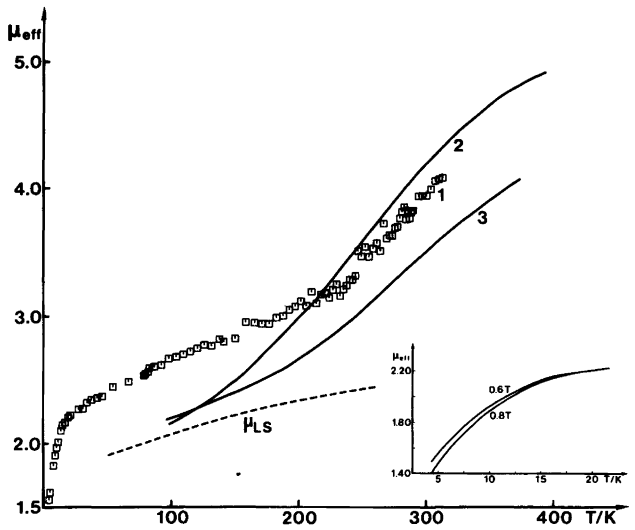

Fig. 4. The effective magnetic moment of $Fe[S_2CN(C_3H_4N)_2]_3 \cdot \frac{1}{2}CHCl_3$ (*1*) as a function of temperature compared with the corresponding curves for $Fe[S_2CN(CH_3)_2]_3$ (*2*) and $Fe[S_2CN(CH_2C_6H_5)_2]_3$ (*3*). The inset shows the effect of the external field when $T < 20$ K.

approximately should equal the mean decrease in unit cell dimensions. We find $\Delta(V^{1/3}) = 0.067(3)$ Å in rather good agreement with $\Delta + 2\delta(Fe-S) = 0.078(6)$ Å.

MAGNETIC PROPERTIES AND THE NATURE OF THE SPIN TRANSITION

Fig. 4 shows the effective magnetic moment μ_{eff} as a function of temperature (μ_{eff} is the number of Bohr magnetons; 1 B M $= 9.274 \cdot 10^{-24}$ J T^{-1}). The plot can be divided into three parts: (*i*) $T > 225$ K, (*ii*) $20\text{ K} < T < 225$ K and (*iii*) $T < 20$ K. Above 225 K the

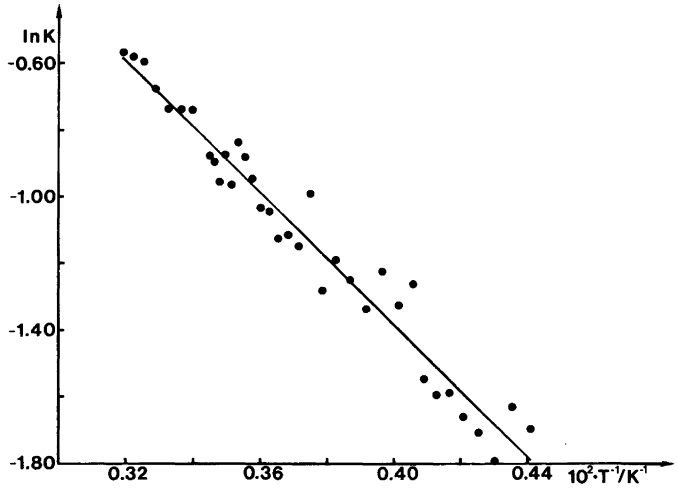

Fig. 5. A plot of ln K *vs.* T^{-1} ($T > 225$ k) where $K = x_{HS}/(1 - x_{HS})$ and x_{HS} the fraction of the complexes in high-spin state.

plot is intermediate to that of the methyl substituted iron(III) dithiocarbamate complex ($pK_a = 11.9$ for dimethylamine[9]) and that of the benzyl substituted ($pK_a = 8.5$ for dibenzylamine[20]). Obviously the inductive effect from the substituents is of minor importance compared to steric factors, crystal defects and other solid state effects.

We presume that above 225 K we have an equilibrium between high and low-spin complexes. We denote the fraction of high-spin complexes with x_{HS} defined by eqn. (2), where $\mu^2_{HS} = 35$ and μ^2_{LS} as given in eqn. (3) with $y = \lambda/RT$ and $\lambda = -5000$ J

$$\mu^2_{eff} = x_{HS}\mu^2_{HS} + (1 - x_{HS})\mu^2_{LS} \quad (2)$$

$$\mu^2_{LS} = \frac{8 + (3y - 8)e^{-3y/2}}{y(2 + e^{-3y/2})} \quad (3)$$

mol^{-1}.[21] The trigonal distortion of the complex will only cause minor deviations in μ_{LS} compared to eqn. (3) above ~100 K.[22] A simple thermodynamic treatment of the crossover region $T > 225$ K is shown in Fig. 5, where ln K is plotted *vs.* T^{-1}. $K = x_{HS}/(1 - x_{HS})$ is the formal equilibrium constant for the $S = \frac{1}{2} \rightleftarrows S = \frac{5}{2}$ transition. The spin equilibrium is independent of the disorder $A \rightleftarrows B$ discussed above. Following Ref. 23 we evaluate the straight line in Fig. 5 using eqn. (1). The resulting effective changes in enthalpy and entropy are related to the standard changes by $\Delta H_{eff} = n\Delta H^\circ$ and $\Delta S_{eff} = n\Delta S^\circ$. The quantity n is a function of the intermolecular interactions, sometimes expressed as a domain size. ΔH_{eff} and ΔS_{eff} are then changes associated with the transition of 1 mol LS domains to HS domains, each domain containing n complexes. The line in Fig. 5 gives us $\Delta H_{eff} = 8.4(3)$ kJ mol^{-1} and $\Delta S_{eff} = 22(1)$ J K^{-1} mol^{-1}. The spin contribution to ΔS° is $R \cdot \ln(2 \cdot \frac{5}{2} + 1)/(2 \cdot \frac{1}{2} + 1) = 9.1$ J K^{-1} mol^{-1} and the contributions from intermolecular and lattice vibrations are positive.[23] We conclude that ΔS_{eff} and ΔS° are of the same order of magnitude and set an upper limit of n to ~2. Repeated measurements after careful grinding of the sample gave the same result. Thus, the spin transition appears to be non-cooperative in the region above 225 K. The appreciable amount of $A \rightleftarrows B$ disorder in this range and the solvate molecules give almost one site per complex for nucleation of a spin-changed domain.

Since the disorder and spin transition are similarly affected by the temperature ($x_B \approx x_{HS}$ at 225 and 300 K) the two processes show approximately the same enthalpy and entropy changes.

At 225 K and below there is a residual occupancy of the high-spin state; $x_{HS} = 0.15$ at 225 K, which slowly decreases as the temperature is lowered. In this low-temperature region there are small thermal vibration amplitudes and little occurrence of $A \rightleftarrows B$ disorder. The effect of the solid state on the spin transition may be quite different here compared to the high-temperature region. However, the main part of the decrease in effective magnetic moment in part (*ii*) of the μ_{eff} *vs.* T plot is the decrease in the value of μ_{LS}. The dashed curve in Fig. 4 shows μ_{LS} *vs.* T using eqn. (3).

The sharp decrease in μ_{eff} below 20 K is as can be expected from more complete calculations of the magnetic properties of the d^5 electron system made by Figgis[22] and König and Kremer.[24] The effect should be further enhanced by zero field splitting caused by the trigonal distortion of the FeS_6 core from O_h symmetry.[21] There is a noticeable effect on μ_{eff} from the external magnetic field when $T < 15$ K as can be seen in the inset of Fig. 4.[24].

Acknowledgements. We are indebted to Dr. Mats Nygren, University of Stockholm, for many discussions during the construction of the Faraday balance and to Ms. Lena Timby for help with part of the experimental work and for preparation of the illustrations. The Swedish Natural Science Research Council gave financial support.

REFERENCES

1. White, A. H., Roper, R., Kokot, E., Waterman, H. and Martin, R. L. *Aust. J. Chem. 17* (1964) 294.
2. Ewald, A. H., Martin, R. L., Sinn, E. and White, A. H. *Inorg. Chem. 8* (1969) 1837.
3. Albertsson, J., Elding, I. and Oskarsson, Å. *Acta Chem. Scand. A 33* (1979) 703.
4. Albertsson, J., Oskarsson, Å., Ståhl, K., Svensson, C. and Ymén, I. *Acta Crystallogr. B 37* (1981) 50.
5. Leipoldt, J. G. and Coppens, P. *Inorg. Chem. 12* (1973) 2269.
6. Haddad, M. S., Lynch, M. W., Federer, W. D. and Hendrickson, D. N. *Inorg. Chem. 20* (1981) 123.
7. Haddad, M. S., Federer, W. D., Lynch, M. W. and Hendrickson, D. N. *Inorg. Chem. 20* (1981) 131.
8. Stevensson, G. W. and Williamson, D. *J. Am. Chem. Soc. 80* (1958) 5943.

9. Everett, D. H. and Wynne-Jones, W. F. K. *Proc. R. Soc. London A 177* (1941) 499.
10. Danielsson, S., Grenthe, I. and Oskarsson, Å. *J. Appl. Crystallogr. 9* (1976) 14.
11. Bodforss, S. *Kungl. Fysiogr. Sällsk. Lund Förh. 7* (1938) No. 16.
12. Blom, B. and Hörlin, T. *Chem. Commun. Univ. Stockholm* (1977) No. 5.
13. Mulay, L. N. and Mulay, I. N. *Anal. Chem. 46* (1974) 4912.
14. Main, P., Hull, S. E., Lessinger, L., Germain, G., Declercq, J.-P. and Woolfson, M. M. *MULTAN, A Program for the Automatic Solution of Crystal Structures from X-Ray Diffraction Data*, Univs. of York, England and Louvain, Belgium, 1978; Woolfson, M. M. *Acta Crystallogr. A 33* (1977) 219.
15. *International Tables for X-Ray Crystallography*, Kynoch Press, Birmingham 1974, Vol. 4.
16. Abrahams, S. C. and Keve, E. T. *Acta Crystallogr. A 27* (1971) 157.
17. Ståhl, K. and Ymén, I. *To be published;* Oskarsson, Å., Ståhl, K. and Ymén, I. *Abstract to XXII ICCC*, Budapest 1982, August 23rd – 27th.
18. Albertsson, J. and Oskarsson, Å. *Acta Crystallogr. B 33* (1977) 1871.
19. Barrow, M. I. *Acta Crystallogr. B 37* (1981) 2239.
20. Christensen, J. J., Izatt, R. M., Wranthall, D. P. and Hansen, L. D. *J. Chem. Soc. A* (1969) 1212.
21. Ballhausen, C. J. *Introduction to Ligand Field Theory*, McGraw-Hill, New York 1962, pp. 111 – 149.
22. Figgis, B. N. *Trans. Faraday Soc. 57* (1961) 204.
23. Gütlich, P., Köppen, H., Link, R. and Steinhäuser, H. G. *J. Chem. Phys. 70* (1979) 3977.
24. König, E. and Kremer, S. *Ber. Bunsenges. Phys. Chem. 78* (1974) 269.

Received March 22, 1982.